A Unity Power Factor Active Rectifier with Optimum Space-Vector Predictive DC Voltage Control for Variable Frequency Supply Suitable for More Electric Aircraft Applications

Joseph Benzaquen*, Mohammad B. Shadmand*, Arlie Stonestreet II†, and Behrooz Mirafzal*
*Electrical and Computer Engineering Department, Kansas State University, Manhattan, KS 66506 USA
†Ultra Electronics ICE, Inc., USA
jbenzaquen@ksu.edu; mshadmand@ksu.edu; Arlie.Stonestreet@Ultra-ICE.com; mirafzal@ksu.edu

***Abstract*—Power electronic converters are the enabling technology and the future of More Electric Aircraft (MEA). One of the major changes in MEA is that the main ac-bus frequency varies over a wide range (360-800Hz). Thus, for MEA applications the power electronic converters must operate under wild frequency conditions. In this paper, a three-phase unity power factor (UPF) active rectifier with optimum space-vector predictive dc voltage control (OSVP) for variable frequency supply is presented. The proposed controller takes into account the supply's frequency change by means of an instantaneous phase-locked-loop (PLL). Furthermore, only an *L* filter is required to meet the current distortion levels due to the high switching frequency of modern semiconductors and the fast response time of the proposed controller. The system is analyzed under load step changes as well model mismatch to demonstrate the validity and performance of the proposed OSVP control under variable frequency. Finally, the classical PI-based PQ-control scheme is used as a reference to benchmark the performance of the proposed control scheme. Though, both controllers perform similarly in terms of current Total Harmonic Distortion (THD), dc voltage regulation, and transient response, the OSVP control scheme has a simpler and more compact filter (i.e. *L* filter instead of an *LCL* filter), and stability index.**

I. Introduction

The next generation of commercial passenger and military airplanes power systems will be significantly impacted by the implementation of the More Electric Aircraft (MEA) technologies. Multiple functions that are traditionally operated by hydraulic, pneumatic, or mechanical power will be electrified in order to reduce the size and weight, and improve fuel efficiency [1], [2]. It is estimated that an MEA design can reduce the aircraft weight by 10% and fuel consumption by 9% [3]. In this sense, aviation standards such as the MIL-STD-704F [4] and DS-160 provide strict regulations for the MEA power systems, such as, current Total Harmonic Distortion (THD) levels, as well as, dc and ac steady-state voltage operational limits. In order to comply with these regulations, future MEA will require state-of-the-art power electronic converters. The recent developments in Wide Bandgap (WBG) semiconductors will aid in the technological transition as they allow the design of compact and efficient converters given their high switching frequency capabilities and low switching and conduction loses [5].

An MEA power grid is a hybrid ac/dc system. The main bus has a constant voltage and variable frequency ($360 - 800\,\mathrm{Hz}$) voltage generated by the synchronous generators that are directly coupled to the main jet engines [2], [6], [7]. To generate a dc voltage, a multi-pulse (12 or 18 pulse) passive autotransformer rectifier unit (ATRU) is used [1]. While those are reliable and extensively implemented in current aircraft power systems, the ATRU still produces high order odd non-triplen harmonics and does not operate at a unity power factor. As a first approach to minimize the harmonics injected to the system by the ATRU, an active power filter (APF) can be implemented at the main bus as suggested in [2], [8]–[10]. A second alternative is to replace the ATRU by a PWM-based active rectifier. While active rectifiers are a well known topic in the literature [11]–[13], their design, control, and performance for high and variable fundamental frequency ($360 - 800\,\mathrm{Hz}$) applications is still an active research topic.

In [14]–[16], the focus of the controller is centered around the permanent magnet synchronous generator (PMSG) which is directly coupled with the main jet engines. This imposes additional complexity to the controller since it needs to consider the PMSG dynamics. Direct ac-ac matrix converters can also be implemented in conjunction with the ATRU as proposed in [17]. To meet the THD requirements, this converter uses both input and output single-stage LC filters, which add volume and reduce the overall efficiency. In [7], it is shown that a six-switch three-level Vienna Type rectifier [18] is well suited for variable frequency MEA applications where the ac mains voltage level is set to $115\,\mathrm{V} \pm 15\%$. However, for the new MEA systems in which the ac-bus voltage will be increased to $230\,\mathrm{V}$, the three-level three-phase rectifier topologies show greater efficiency given the decrease of the conduction losses as presented in [19]. For all the previous converter designs, the standard six-switch PWM active rectifier is not taken into account due to its (i) high switching and conduction losses, (ii) bidirectional power flow behavior, and (iii) controller complexity.

978-1-5386-1180-7/18/$31.00 ©2018 IEEE

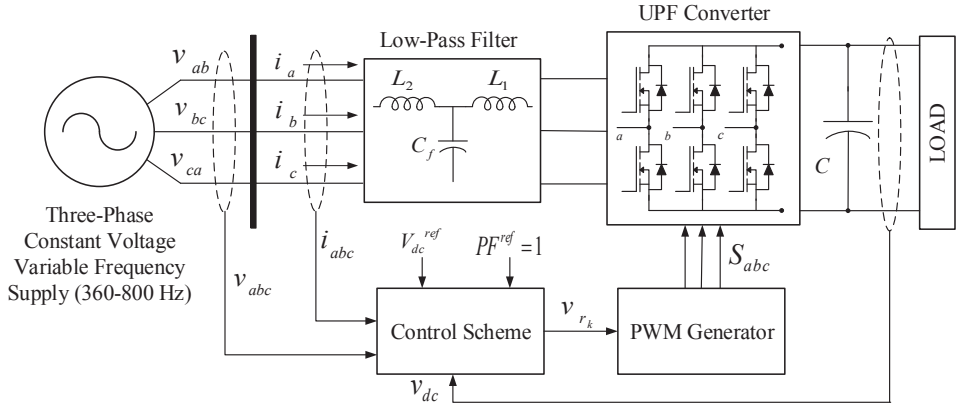

Fig. 1. Block diagram of a general three-phase unity power factor active rectifier.

In this paper, a three-phase unity power factor (UPF) active rectifier with optimum space-vector predictive dc voltage control (OSVP) is presented. The voltage is regulated with only one PI control loop which gives the active power reference to the OSVP algorithm, while the reactive power reference can be directly set in the algorithm; thus avoiding the complexity and tuning of multi-PI current- or voltage-source control schemes. Furthermore, the OSVP controller allows the direct control of the active power drawn from the source ensuring unidirectional operation. The proposed system requires only a simple L input filter to maintaining the current THD level under 5%. As a consequence, resonance problems, damping techniques, phase-shifting, as well as additional losses can be avoided [20]. In order to operate with a variable frequency supply that can change at any rate as required by a MEA, an instantaneous Phase-Locked Loop (PLL) [21] is implemented in conjunction with the OSVP algorithm. The instantaneous PLL can respond with minimum delay to the frequency changes and does not require tuning as opposed to the classical PI-based PLLs [22].

In addition to this introduction, this paper contains four sections . In Section II, a brief description of the MEA power system is given. In Section III, the proposed OSVP control scheme is derived and explained. Matlab/Simulink simulation results demonstrating the performance of the proposed technique, are provided in Sections IV. Finally, in Section V a summarizes the findings of this paper.

II. MEA Power System Description

The power system of an aircraft is designed to supply both dc and ac loads at different voltage levels. A set of synchronous generators connected to the main jet engines via a mechanical drive generate a constant voltage at a fixed frequency of $400\,\text{Hz}$ in most aircraft legacy models. In some of the recent commercial transport MEA, such as Boeing 787 and Airbus A380, the electric generators are directly coupled to the jet engines. Thus, generating a constant main ac voltage bus at a variable frequency that ranges between $360-800\,\text{Hz}$. This variable frequency configuration has been standardized for MEA in the MIL-STD-704 and DS-160 [6].

In the majority of MEA power systems, the main variable frequency bus feeds three types of systems (i) $115\,\text{V}/200\,\text{V}$ ac with a variable frequency between $360-800\,\text{Hz}$, (ii) $28\,\text{V}$ dc, and (iii) $270\,\text{V}$ dc. These systems supply all the load of the aircraft, which is approximately distributed as fallows: 40% supplied by the ac variable frequency buses, 40% by the $270\,\text{V}$ dc-bus, and 10% by the $28\,\text{V}$ dc-bus. The reminder 10% is considered as total losses [23].

III. Optimum Space-Vector Predictive DC Voltage Control

The general structure of a three-phase unity power rectifier is depicted in Fig. 1. This converter controls the dc-bus voltage while maintaining a unity power factor in the ac side. As with any power electronic converter, the high-order harmonics generated by the switching of the semiconductor components needs to be attenuated by a passive low-pass filter. This configuration serves as the foundation for the OSVP dc voltage control, which is based on the estimation of the state variables of the system at sampling time $k+1$ to determine the next

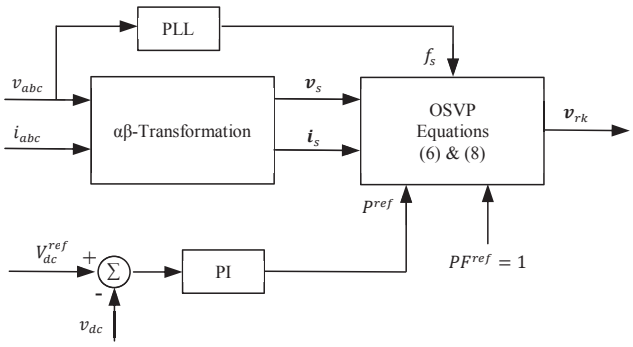

Fig. 2. OSVP control block diagram.

control action based on the measurements taken at the previous k instant. [24]–[30]. For an UPF active rectifier, the control variables are the dc voltage and the reactive power. Since the controller equations are based in the active and reactive instantaneous power, an additional PI controller is added to regulate the dc voltage through the correct setting of the active power reference. As a result, the main objective of the controller scheme is to determine the optimum voltage space-vector that the converter should generate to minimize the error between the measured and reference active and reactive power for the future control cycle.

The OSVP control uses an inductor or L filter as a low-pass filter. Thus, simplifying the modeling of the system. A single complex differential equation in the $\alpha\beta$ in the stationary reference frame [31], [32] models the system as described in (1).

$$\boldsymbol{v}_s = \boldsymbol{v}_r + R_f \boldsymbol{i}_s + L_f \frac{\mathrm{d}\boldsymbol{i}_s}{\mathrm{d}t} \tag{1}$$

Where, $\boldsymbol{v}_s$ is the ac supply phase-to-neutral voltage space-vector, $\boldsymbol{v}_r$ is the rectifier phase-to-neutral voltage space-vector, $\boldsymbol{i}_s$ is the line current space-vector, and R_f and L_f are the parameters of the L filter. The voltage and current space-vectors are computed using the power-invariant coordinate transformation $\alpha\beta$ in the stationary reference frame . From (1), the ac line current at the next control cycle $\boldsymbol{i}_{s_{k+1}}$ can be estimated using a Forward Euler discrete approximation considering the control sampling time T_s as fallows:

$$\boldsymbol{i}_{s_{k+1}} = \boldsymbol{i}_{s_k} + \left(\frac{T_s}{L_f}\right)\left(\boldsymbol{v}_{s_k} - \boldsymbol{v}_{r_k} - R_f \boldsymbol{i}_{s_k}\right). \tag{2}$$

The use of a power-conservative space-vector transformation allows the calculation of the instantaneous three-phase active (p) and reactive (q) power from $s = \boldsymbol{v}_s \boldsymbol{i}_s^* = p + jq$. Consequently, the variation of p and q from the control cycle k to $k+1$ can be written as function of $\boldsymbol{v}_s$ and $\boldsymbol{i}_s$ as

$$\begin{aligned} \Delta s_k &= s_{k+1} - s_k \\ &= \boldsymbol{v}_{s_{k+1}} \boldsymbol{i}^*_{s_{k+1}} - \boldsymbol{v}_{s_k} \boldsymbol{i}^*_{s_k}. \end{aligned} \tag{3}$$

In (3), $\boldsymbol{v}_{s_{k+1}}$ can be estimated for a balanced three-phase sinusoidal voltage supply by rotating $\boldsymbol{v}_{s_k}$ in ωT_s radians (i.e. $\boldsymbol{v}_{s_{k+1}} = \boldsymbol{v}_{s_k} e^{j\omega T_s}$), where ω is the angular frequency of the supply in $\mathrm{rad/s}$, which can be estimated by a classical three-phase PLL [22], [33]. Nonetheless, given the fast changes in the frequency, an instantaneous PLL such as the one proposed in [21] is implemented as part of the OSVP control scheme. The frequency estimation is based on the following expression:

$$\omega = \frac{\mathrm{d}}{\mathrm{d}t}\left[\arctan\left(\frac{v_{ab} + 2v_{bc}}{\sqrt{3}v_{ab}}\right)\right]. \tag{4}$$

By substituting (2) into (3), the change in apparent power, Δs_k, can be written as

$$\Delta s_k = \Delta s_0 - \left(\frac{T_s}{L_f}\right) e^{j\omega T_s} \boldsymbol{v}_{s_k} \boldsymbol{v}^*_{r_k}, \tag{5}$$

where,

$$\Delta s_0 = \left(\frac{T_s}{L_f}\right) e^{j\omega T_s} \left|\boldsymbol{v}_{s_k}\right|^2 + \boldsymbol{v}_{s_k} \boldsymbol{i}^*_{s_k} \left[e^{j\omega T_s}\left(1 - \frac{R_f}{L_f} T_s\right) - 1\right]. \tag{6}$$

For any given active (p_{ref}) and reactive (q_{ref}) power reference, the apparent power , Δs_k, represents the power needed to change from the actual p_k and q_k values to their respective references in the following control cycle. In order to compute the optimum space-vector to achieve the desired reference power, Δs_k should equal the difference between the reference and calculated power as shown in (7).

$$(p_{ref} - p_k) + j\,(q_{ref} - q_k) = \Delta s_k \tag{7}$$

By replacing (5) into (7), the optimum rectifier voltage, $\boldsymbol{v}_{r_k}$, required to generate the desired active and reactive power is

$$\boldsymbol{v}_{r_k} = \left(\frac{L_f}{T_s}\right)\left[\frac{\Delta s_0 - (p_{ref} - p_k) - j\,(q_{ref} - q_k)}{\boldsymbol{v}_{s_k} e^{j\omega T_s}}\right]^*. \tag{8}$$

The voltage space-vector obtained in (8) is the optimum voltage vector that will produce the desired active and reactive power in the next control step. Finally, $\boldsymbol{v}_{r_k}$ is synthesized using space-vector modulation (SVPWM) [34]. The OSVP control block diagram is depicted in Fig. 2.

IV. Results & Analysis

A digital computer simulation using Matlab/Simulink was used to demonstrate the validity and performance of the OSVP controller. In addition, the OSVP control was compared to an LCL filter PQ-control active rectifier. The general system configuration used for both controllers is shown in Fig. 1. The parameters of the system for each case are detailed in Table I.

TABLE I
Simulation parameters for the OSVP and PQ-control

Param.	OSVP	PQ-control	Param.	OSVP	PQ-control
L_1	$480\,\mu$H	$150\,\mu$H	R_1	$0.5\,\Omega$	$0.25\,\Omega$
L_2	-	$330\,\mu$H	R_2	-	$0.25\,\Omega$
C_f	-	$0.27\,\mu$F	R_{C_f}	-	$1.1\,\Omega$
f_{PWM}	50 kHz	50 kHz	C	$100\,\mu$F	$100\,\mu$F
Q_{ref}	0	0			

A. Instantaneous PLL and Classical PLL Comparison for OSVP

The frequency of the main ac-bus in an MEA is dictated by the speed of the jet engines. To take into account for rapid changes in the supply frequency the proposed OSVP control implements an instantaneous PLL [21] based on (4). Fig. 3 shows the advantages of implementing an instantaneous PLL as opposed to a classical PI-based PLL. In Fig. 3(a), the performance of the instantaneous PLL and a classical PLL is depicted for a wild frequency profile f_s. The classical PLL is design to damp the rapid variations in frequency since

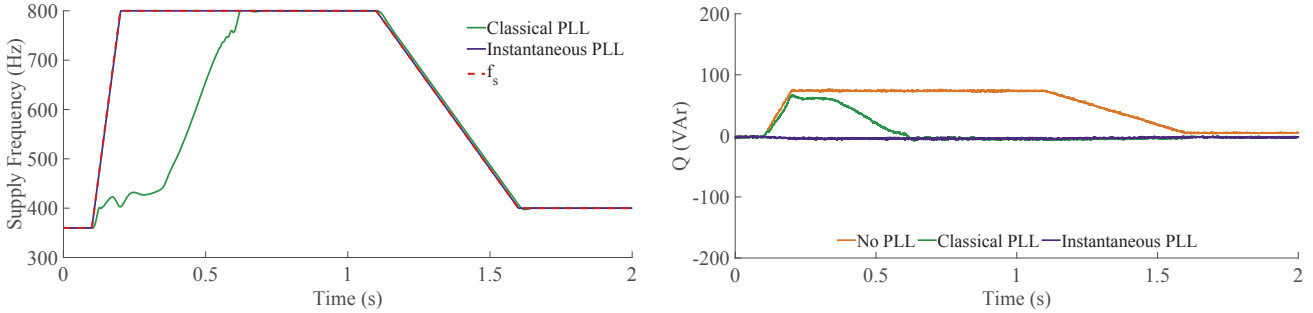

Fig. 3. PLL comparison for a variable supply frequency profile with OSVP control. (a) PLL frequency estimation. (b) average reactive power regulation for the different PLLs.

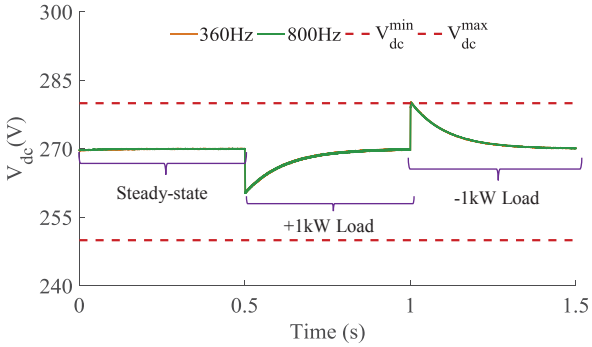

Fig. 4. Regulation of the dc-bus voltage with load step changes.

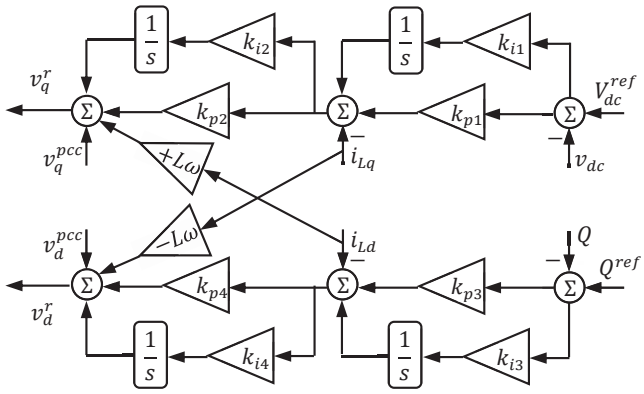

Fig. 5. PQ-control block diagram.

in a conventional system the inertia of the generator will not permit quick frequency changes. Consequently, for MEA applications, where the frequency variation can be higher that in conventional systems, a classical PLL must be properly tuned to estimate the frequency. With the implementation of the instantaneous PLL, no tuning is required and the frequency can be estimated in real time as shown in Fig. 3(a). Finally, in Fig. 3(b) demonstrates the effects on the controlled reactive power of the OSVP control scheme for three scenarios (i) no PLL, classical PLL, and instantaneous PLL.

B. Transient Performance for Load Step Changes

The transient performance of the OSVP under load step changes is depicted in Fig. 4. After the system reaches steady-state at 50% load, the dc load was doubled to 100% at $t = 0.5\,\text{s}$. Finally, at $t = 1\,\text{s}$, the load is dropped back to 50%. A voltage sag and swell can be observed when the load is increased and decreased for the minimum operating frequency (360 Hz) as well as the maximum operating frequency (800 Hz). In both cases, the dc voltage level complies with the MIL-STD-704F standard [4].

C. Model Mismatch Tolerance

The OSVP dc-bus control can be categorized as a Model Predictive Control (MPC) [24], [25]. As such, the stability and performance of the controller is dependent on any model mismatch that may occur from any variation of a component on the circuit. In the case of an L filter, the parameter variations may be caused by temperature variations, core saturation, fringing, skin effect, etc. In this sense, the resistance and inductance variation effects on the performance of the controller must be analyzed.

TABLE II
EFFECT ON THE CONTROLLED REACTIVE POWER AS FUNCTION OF L_f INDUCTANCE VARIATIONS AT DIFFERENT SUPPLY FREQUENCIES

L_f	300 Hz	400 Hz	500 Hz	600 Hz	700 Hz	800 Hz
0%	1.01%	1.33%	1.68%	1.97%	2.98%	2.76%
±10%	1.65%	1.99%	2.53%	3.02%	3.60%	3.94%
±20%	2.01%	2.64%	3.31%	3.98%	4.81%	5.17%
±30%	2.58%	3.28%	4.11%	4.98%	5.75%	6.41%

In Table II, the effect of the filter variation on the controlled reactive power is presented for different frequencies. While the variation of L_f does not make the system unstable, it can impact the unity power factor operation of the system. As expected, the reactive power error or deviation from the reference set point ($Q_{ref} = 0$) increases as the frequency of the supply increases, reaching up to almost 10% for 800 Hz and an inductance variation of ±50%. Contrary to L_f, the variation of the inherent resistance of the filter, R_f, can make

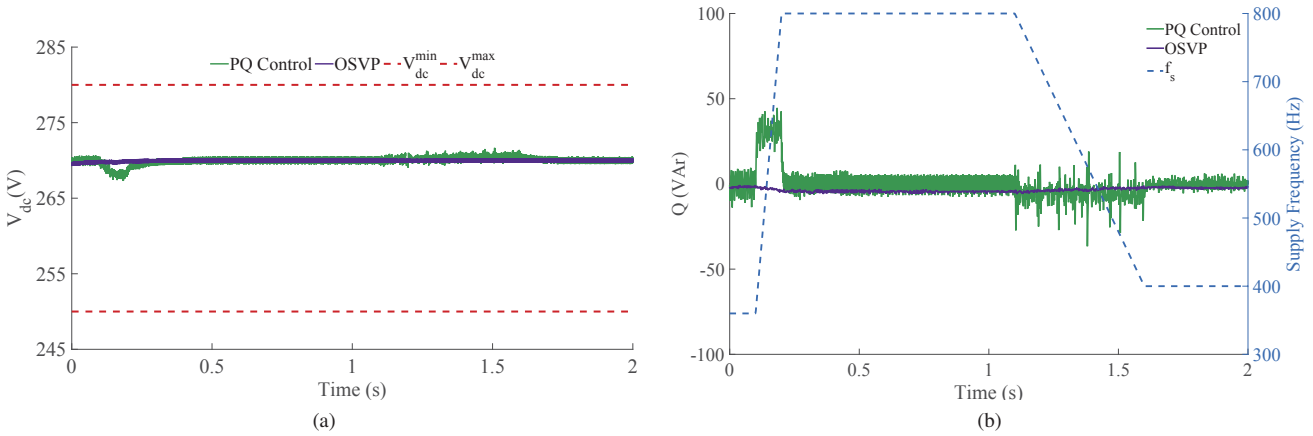

Fig. 6. OSVP and PI-based PQ control comparison for a variable supply frequency profile. (a) dc voltage regulation for the 270 V bus. (b) average reactive power regulation and supply frequency profile.

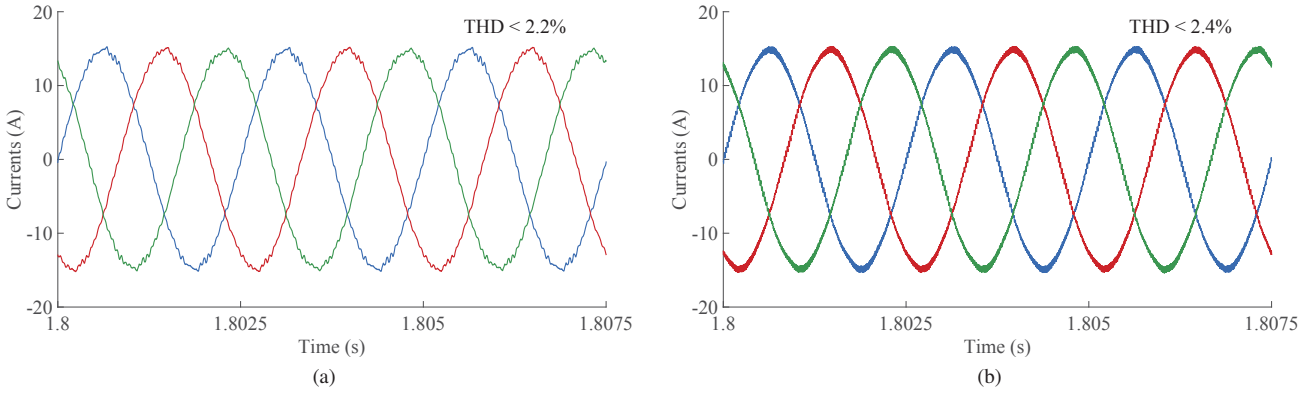

Fig. 7. OSVP and PI-based current control comparison. (a) PQ control currents at 400 Hz. (b) OSVP control currents at 400 Hz.

the system unstable. Table III depicts the maximum values that R_f can variate for a given supply frequency before the system becomes unstable.

TABLE III
R_f PARAMETER VARIATION TOLERANCE FOR STABLE OPERATION AT DIFFERENT SUPPLY FREQUENCIES

Frequency (Hz)	R_f variation	Frequency (Hz)	R_f variation
300	$\pm 10\%$	600	$\pm 37\%$
400	$\pm 20\%$	700	$\pm 42\%$
500	$\pm 29\%$	800	$\pm 55\%$

D. OSVP and PI-based Current Control Comparison

In order to adequately evaluate the performance of the OSVP control scheme, the proposed control technique was compared with a PI-based LCL filter current control (see Fig. 5). This controller can serve as an effective benchmark for comparison given its popularity and high industrial implementation. To establish a fair comparison, both control schemes used the instantaneous PLL described in [21]. Fig. 6 depicts the performance of both controllers for a wild frequency supply profile. As can be seen in Fig. 6, both controllers effectively regulate the dc voltage bus while operating at a unity power factor. In addition, for the two control schemes, the line current THD is below 2.4%, as shown in Fig. 7.

V. Conclusions

In this paper a three-phase UPF active rectifier with OSVP for variable frequency ac supply suitable for MEA applications has been presented. The rapid changes in the main ac-bus due to the jet engine speed variations was taken into account by implementing an instantaneous PLL as opposed to the classical PI-based PLL. The proposed control scheme was verified and analyzed Matlab/Simulink simulation. A wild frequency profile consisting of one acceleration and one deceleration ramp was used to evaluate the performance of the controller with different PLLs and then compared to a classical PI-based LCL filter current control. The simulation results demonstrate that combined the instantaneous PLL and the OSVP control can effectively regulate the dc-bus while maintaining a unity power factor in the ac lines. Furthermore, when compared to the classical PI-based LCL PQ-control scheme, the OSVP shows a similar performance in terms of current THD, dc voltage

regulation, and reactive power regulation. This is accomplished by the OSVP control by using one L filter, and one PI control loop for the dc voltage as opposed to an LCL filter and four PI control loops. Moreover, the proposed controller can regulate the dc voltage with step load changes while complying with MIL-STD-704F standard. Finally, as a tool for the design and implementation of the OSVP controller for MEA applications, a model mismatch analysis was presented. Both the variations of the resistance and inductance of the L filter were analyzed for different supply frequencies. While the inductance variation can only affect the reactive power control, it was demonstrated that the resistance variation can affect the stability of the system, specially at low supply frequencies.

REFERENCES

[1] J. Sun, Z. Bing, and K. J. Karimi, "Small-signal modeling of multipulse rectifiers for more-electric aircraft applications," in *2008 IEEE Power Electronics Specialists Conference*, Jun. 2008, pp. 302–308.

[2] J. Chen, X. Zhang, and C. Wen, "Harmonics attenuation and power factor correction of a more electric aircraft power grid using active power filter," *IEEE Trans. Ind. Electron.*, vol. 63, no. 12, pp. 7310–7319, Dec. 2016.

[3] K. Rajashekara, "More electric aircraft trends [Technology Leaders]," *IEEE Electrific. Mag.*, vol. 2, no. 4, pp. 4–39, Dec. 2014.

[4] "Aircraft electric power characteristics," *Department of Defense Interface Standard (MIL-STD-704F)*, 2004.

[5] J. Millán, P. Godignon, X. Perpiñà, A. Pérez-Tomás, and J. Rebollo, "A survey of wide bandgap power semiconductor devices," *IEEE Trans. Power Electron.*, vol. 29, no. 5, pp. 2155–2163, May 2014.

[6] B. Sarlioglu and C. T. Morris, "More electric aircraft: Review, challenges, and opportunities for commercial transport aircraft," *IEEE Trans. Transport. Electrific.*, vol. 1, no. 1, pp. 54–64, Jun. 2015.

[7] G. Gong, M. L. Heldwein, U. Drofenik, J. Minibock, K. Mino, and J. W. Kolar, "Comparative evaluation of three-phase high-power-factor AC-DC converter concepts for application in future more electric aircraft," *IEEE Trans. Ind. Electron.*, vol. 52, no. 3, pp. 727–737, Jun. 2005.

[8] Z. Chen, Z. Wang, and M. Chen, "Four hundred hertz shunt active power filter for aircraft power grids," *IET Power Electron.*, vol. 7, no. 2, pp. 316–324, Feb. 2014.

[9] S. Liebig and J. Lutz, "Efficiency and lifetime of an active power filter with SiC-MOSFETs for aerospace application," in *PCIM Europe 2014; International Exhibition and Conference for Power Electronics, Intelligent Motion, Renewable Energy and Energy Management*, May 2014, pp. 1–9.

[10] E. Lavopa, P. Zanchetta, M. Sumner, and F. Cupertino, "Real-time estimation of fundamental frequency and harmonics for active shunt power filters in aircraft electrical systems," *IEEE Trans. Ind. Electron.*, vol. 56, no. 8, pp. 2875–2884, Aug. 2009.

[11] B. Singh, B. N. Singh, A. Chandra, K. Al-Haddad, A. Pandey, and D. P. Kothari, "A review of three-phase improved power quality AC-DC converters," *IEEE Trans. Ind. Electron.*, vol. 51, no. 3, pp. 641–660, Jun. 2004.

[12] J. W. Kolar and T. Friedli, "The essence of three-phase PFC rectifier systems - part I," *IEEE Trans. Power Electron.*, vol. 28, no. 1, pp. 176–198, Jan. 2013.

[13] T. Friedli, M. Hartmann, and J. W. Kolar, "The essence of three-phase PFC rectifier systems - part II," *IEEE Trans. Power Electron.*, vol. 29, no. 2, pp. 543–560, Feb. 2014.

[14] Z. Xu, D. Zhang, F. . Wang, and D. Boroyevich, "A unified control for the combined permanent magnet generator and active rectifier system," *IEEE Trans. Power Electron.*, vol. 29, no. 10, pp. 5644–5656, Oct. 2014.

[15] D. M. Miao, Y. Mollet, J. Gyselinck, and J. X. Shen, "DC voltage control of a wide-speed-range permanent-magnet synchronous generator system for more electric aircraft applications," in *2016 IEEE Vehicle Power and Propulsion Conference (VPPC)*, Oct. 2016, pp. 1–6.

[16] F. Gao, X. Zheng, S. Bozhko, C. I. Hill, and G. Asher, "Modal analysis of a PMSG-based DC electrical power system in the more electric aircraft using eigenvalues sensitivity," *IEEE Trans. Transport. Electrific.*, vol. 1, no. 1, pp. 65–76, Jun. 2015.

[17] S. L. Arevalo, P. Zanchetta, P. W. Wheeler, A. Trentin, and L. Empringham, "Control and implementation of a matrix-converter-based AC ground power-supply unit for aircraft servicing," *IEEE Trans. Ind. Electron.*, vol. 57, no. 6, pp. 2076–2084, Jun. 2010.

[18] J. W. Kolar and F. C. Zach, "A novel three-phase utility interface minimizing line current harmonics of high-power telecommunications rectifier modules," *IEEE Trans. Ind. Electron.*, vol. 44, no. 4, pp. 456–467, Aug. 1997.

[19] M. Hartmann, J. Miniboeck, H. Ertl, and J. W. Kolar, "A three-phase delta switch rectifier for use in modern aircraft," *IEEE Trans. Ind. Electron.*, vol. 59, no. 9, pp. 3635–3647, Sep. 2012.

[20] L. Shen, G. Asher, P. Wheeler, and S. Bozhko, "Optimal LCL filter design for 3-phase space vector PWM rectifiers on variable frequency aircraft power system," in *2013 15th European Conference on Power Electronics and Applications (EPE)*, Sep. 2013, pp. 1–8.

[21] D. S. Ochs, B. Mirafzal, and P. Sotoodeh, "A method of seamless transitions between grid-tied and stand-alone modes of operation for utility-interactive three-phase inverters," *IEEE Trans. Ind. Appl.*, vol. 50, no. 3, pp. 1934–1941, May 2014.

[22] S. Golestan, J. M. Guerrero, and J. C. Vasquez, "Three-phase PLLs: A review of recent advances," *IEEE Trans. Power Electron.*, vol. 32, no. 3, pp. 1894–1907, Mar. 2017.

[23] R. Abdel-Fadil, A. Eid, and M. Abdel-Salam, "Fuzzy logic control of modern aircraft electrical power system during transient and steady-state operating conditions," in *2014 IEEE International Conference on Power Electronics, Drives and Energy Systems (PEDES)*, Dec. 2014, pp. 1–6.

[24] S. Kouro, P. Cortes, R. Vargas, U. Ammann, and J. Rodriguez, "Model predictive control - A simple and powerful method to control power converters," *IEEE Trans. Ind. Electron.*, vol. 56, no. 6, pp. 1826–1838, Jun. 2009.

[25] J. Rodriguez, J. Pontt, C. A. Silva, P. Correa, P. Lezana, P. Cortes, and U. Ammann, "Predictive current control of a voltage source inverter," *IEEE Trans. Ind. Electron.*, vol. 54, no. 1, pp. 495–503, Feb. 2007.

[26] M. Malinowski, M. Jasinski, and M. P. Kazmierkowski, "Simple direct power control of three-phase PWM rectifier using space-vector modulation (DPC-SVM)," *IEEE Trans. Ind. Electron.*, vol. 51, no. 2, pp. 447–454, Apr. 2004.

[27] P. Cortés, J. Rodríguez, P. Antoniewicz, and M. Kazmierkowski, "Direct power control of an AFE using predictive control," *IEEE Trans. Power Electron.*, vol. 23, no. 5, pp. 2516–2523, Sep. 2008.

[28] P. Cortés, J. Rodríguez, D. E. Quevedo, and C. Silva, "Predictive current control strategy with imposed load current spectrum," *IEEE Trans. Power Electron.*, vol. 23, no. 2, pp. 612–618, Mar. 2008.

[29] J. A. Restrepo, J. M. Aller, J. C. Viola, A. Bueno, and T. G. Habetler, "Optimum space vector computation technique for direct power control," *IEEE Trans. Power Electron.*, vol. 24, no. 6, pp. 1637–1645, Jun. 2009.

[30] A. Berzoy, A. A. S. Mohamed, and O. Mohammed, "Design considerations and predictive direct current control of active regenerative rectifiers for harmonic and current ripple reduction," in *2016 IEEE Applied Power Electronics Conference and Exposition (APEC)*, Mar. 2016, pp. 928–935.

[31] P. C. Krause, O. Wasynczuk, S. D. Sudhoff, and S. Pekarek, *Analysis of electric machinery and drive systems*. John Wiley & Sons, 2013, vol. 75.

[32] J. M. Aller, A. Bueno, and T. Paga, "Power system analysis using space vector transformation," *IEEE Power Eng. Rev.*, vol. 22, no. 8, pp. 64–64, Aug. 2002.

[33] F. Blaabjerg, R. Teodorescu, M. Liserre, and A. V. Timbus, "Overview of control and grid synchronization for distributed power generation systems," *IEEE Trans. Ind. Electron.*, vol. 53, no. 5, pp. 1398–1409, Oct. 2006.

[34] J. Restrepo, J. M. Aller, A. Bueno, V. M. Guzmán, and M. I. Giménez, "Generalized algorithm for pulse width modulation using a two-vectors based technique," *EPE Journal*, vol. 21, no. 2, pp. 30–39, 2011.